Radiology

ORIGINAL RESEARCH • NEURORADIOLOGY

Whole-Brain Functional and Diffusion Tensor MRI in Human Participants with Metallic Orthodontic Braces

Xinyuan Miao, PhD • Yuankui Wu, MD* • Dapeng Liu, PhD • Hangyi Jiang, PhD • David Woods, DMD • Moshe T. Stern, DMD • Nicholas I. S. Blair, BS • Raag D. Airan, MD, PhD • Chetan Bettegowda, MD, PhD • Keri S. Rosch, PhD • Qin Qin, PhD • Peter C. M. van Zijl, PhD • Jay J. Pillai, MD • Jun Hua, PhD*

From the Neurosection, Division of MRI Research, Russell H. Morgan Department of Radiology and Radiological Science, Johns Hopkins University School of Medicine, 707 N Broadway, Baltimore, Md 21205 (X.M., Y.W., D.L., H.J., Q.Q., P.C.M.v.Z., J.H.); F.M. Kirby Research Center for Functional Brain Imaging, Kennedy Krieger Institute, Baltimore, Md (X.M., Y.W., D.L., Q.Q., P.C.M.v.Z., J.H.); Department of Medical Imaging, Nanfang Hospital, Southern Medical University, Guangzhou, P.R. China (Y.W.); Department of Orthodontics and Pediatric Dentistry, University of Maryland School of Dentistry, Baltimore, Md (D.W., M.T.S.); Department of Biomedical Engineering, Johns Hopkins University, Baltimore, Md (N.I.S.B.); Division of Neuroradiology, Russell H. Morgan Department of Radiology and Radiological Science, Johns Hopkins University School of Medicine, Baltimore, Md (R.D.A., J.J.P.); Department of Neurosurgery, Johns Hopkins University School of Medicine, Baltimore, Md (C.B., J.J.P.); Center for Neurodevelopmental and Imaging Research and Department of Neuropsychology, Kennedy Krieger Institute, Baltimore, Md (K.S.R.); and Department of Psychiatry and Behavioral Sciences, Johns Hopkins University School of Medicine, Baltimore, Md (K.S.R.). Received January 11, 2019; revision requested March 8; revision received September 12; accepted September 26. **Address correspondence to** J.H. (e-mail: *jhua@mri.jhu.edu*).

* X.M. and Y.W. contributed equally to this work.

Supported by the National Institutes of Health through grants from the National Institute of Neurological Disorders and Stroke (1R01NS108452), National Institute of Biomedical Imaging and Bioengineering (R21EB023538, P41 EB015909), and Eunice Kennedy Shriver National Institute of Child Health and Human Development (U54 HD079123).

Conflicts of interest are listed at the end of this article.

See also the editorial by Dietrich in this issue.

Radiology 2020; 294:149–157 • https://doi.org/10.1148/radiol.2019190070 • Content codes: MR NR

Background: MRI performed with echo-planar imaging (EPI) sequences is sensitive to susceptibility artifacts in the presence of metallic objects, which presents a substantial barrier for performing functional MRI and diffusion tensor imaging (DTI) in patients with metallic orthodontic material and other head implants.

Purpose: To evaluate the ability to reduce susceptibility artifacts in healthy human participants wearing metallic orthodontic braces for two alternative approaches: T2-prepared functional MRI and diffusion-prepared DTI with three-dimensional fast gradient-echo readout.

Materials and Methods: In this prospective study conducted from February to September 2018, T2-prepared functional MRI and diffusion-prepared DTI were performed in healthy human participants. Removable dental braces with bonding trays were used so that MRI could be performed with braces and without braces in the same participants. Results were evaluated in regions with strong (EPI dropout regions for functional MRI and the inferior fronto-occipital fasciculus for DTI) and minimal (motor cortex for functional MRI and the posterior limb of internal capsule for DTI) susceptibility artifacts. Signal-to-noise ratio (SNR), contrast-to-noise ratio for functional MRI, apparent diffusion coefficient and fractional anisotropy for DTI, and degree of distortion (quantified with the Jaccard index, which measures the similarity of geometric shapes) were compared in regions with strong or minimal susceptibility effects between the current standard EPI sequences and the proposed alternatives by using paired *t* test.

Results: Six participants were evaluated (mean age ± standard deviation, 40 years ± 6; three women). In brain regions with strong susceptibility effects from the metallic braces, T2-prepared functional MRI showed significantly higher SNR (37.8 ± 2.4 vs 15.5 ± 5.3; $P < .001$) and contrast-to-noise ratio (0.83 ± 0.16 vs 0.29 ± 0.10; $P < .001$), whereas diffusion-prepared DTI showed higher SNR (5.8 ± 1.5 vs 3.8 ± 0.7; $P = .03$) than did conventional EPI methods. Apparent diffusion coefficient and fractional anisotropy were consistent with the literature. Geometric distortion was substantially reduced throughout the brain with the proposed methods (significantly higher Jaccard index, 0.95 ± 0.12 vs 0.81 ± 0.61; $P < .001$).

Conclusion: T2-prepared functional MRI and diffusion-prepared diffusion tensor imaging can acquire functional and diffusion MRI, respectively, in healthy human participants wearing metallic dental braces with less susceptibility artifacts and geometric distortion than with conventional echo-planar imaging.

Online supplemental material is available for this article.

With MRI, magnetic susceptibility effects can cause significant image artifacts such as signal reduction and image distortion, especially when using echo-planar imaging (EPI). Such susceptibility artifacts are commonly seen in the presence of metallic objects. Dental fillings and orthodontic braces containing various metals can cause large artifacts extending from the facial region into the brain at EPI (1–3). Orthodontic treatments have become increasingly accessible and are commonly performed in the United States and around the world (see *https://www.aaoinfo.org*). Furthermore, susceptibility artifacts often affect patients undergoing MRI examinations (4,5), especially in regions close to surgical resection cavities, calcified structures, hemorrhages,

Abbreviations

BOLD = blood oxygenation level dependent, DTI = diffusion tensor imaging, EPI = echo-planar imaging, GRE = gradient echo, MPRAGE = magnetization-prepared rapid acquisition gradient-echo, SE = spin echo, SNR = signal-to-noise ratio, 3D = three-dimensional

Summary

T2-prepared blood oxygenation level–dependent functional MRI and diffusion-prepared diffusion tensor imaging with three-dimensional fast gradient-echo readout can significantly reduce susceptibility artifacts commonly seen at conventional echo-planar MRI, especially in the presence of metallic implants.

Key Results

- T2-prepared functional MRI and diffusion-prepared diffusion tensor imaging (DTI) had lower susceptibility artifacts compared with conventional echo-planar MRI and improved signal-to-noise ratio (SNR) in the regions affected by artifacts (functional MRI: 38 vs 16, $P < .001$; DTI: 5.8 vs 3.8, $P = .03$).
- T2-prepared functional MRI and diffusion-prepared DTI showed preserved SNR (functional MRI: 38 vs 37, $P = .38$; DTI: 5.8 vs 5.8, $P = .43$) in brain regions with strong or minimal susceptibility artifacts caused by the metallic braces, whereas the conventional echo-planar imaging methods showed significantly impaired SNR (functional MRI: 16 vs 45, $P = .02$; DTI: 3.8 vs 6.2, $P = .01$) in regions with strong susceptibility effects.
- Geometric distortion was reduced throughout the brain with diffusion-prepared DTI compared with conventional echo-planar imaging methods (measured by significantly increased Jaccard index in diffusion-prepared DTI: 0.95 vs 0.81, $P < .001$).

lesions that contain hemosiderin, and intracranial metallic implants (2,3).

Blood oxygenation level–dependent (BOLD) functional MRI and diffusion tensor imaging (DTI) are two widely used MRI techniques. Currently, EPI is the method of choice for most functional MRI and DTI studies. However, susceptibility artifacts commonly hamper its application. Several other sequences are less sensitive to susceptibility artifacts than EPI (for instance, the three-dimensional [3D] fast gradient-echo [GRE] sequence with short echo time that is commonly used in anatomic examinations such as magnetization-prepared rapid acquisition gradient-echo [MPRAGE]). However, the requirement of a long echo time to generate BOLD and diffusion contrasts during readout precludes the use of such approaches for functional MRI and DTI. Alternatively, however, BOLD and diffusion contrasts can be induced by using spin preparation modules, which separate contrast generation from the readout, thereby opening the possibility to use virtually any sequence for readout. A whole-brain T2-prepared BOLD functional MRI approach (6) was recently demonstrated, which uses a T2-prepared module (7) to induce BOLD contrast, immediately followed by a 3D fast GRE readout with short echo time (<2 msec). T2-prepared BOLD functional MRI showed little susceptibility artifacts throughout the brain, and greater functional sensitivity than did GRE EPI BOLD functional MRI in regions near air-filled cavities in healthy participants (6) and around the lesions containing blood products in presurgical patients (8,9). Similarly, diffusion contrast can be generated by using diffusion preparation modules (10,11). Among the various strategies, a double refocusing diffusion preparation module followed by a 3D fast GRE readout has been commonly adopted (11–13). Studies have shown that this technique can significantly reduce image distortion, and thus provide more reliable diffusion measures in regions with strong susceptibility artifacts at EPI (14).

Here, we apply T2-prepared BOLD functional MRI and diffusion-prepared DTI with 3D fast GRE readout in healthy participants wearing metallic orthodontic braces to evaluate the ability of these techniques to minimize susceptibility artifacts in the presence of metallic implants.

Materials and Methods

Written informed consent was obtained from six healthy participants in this institutional review board–approved and Health Insurance Portability and Accountability Act–compliant study. Inclusion criteria was age 18–100 years, both women and men. Standard exclusion criteria for MRI apply (15). Dental braces without magnetically activated components are considered safe for MRI (15).

Figure 1 illustrates the functional MRI and DTI sequences. The T2-prepared BOLD functional MRI sequence consists of a double refocusing T2-preparation module for generating the BOLD contrast, followed by a 3D fast GRE readout. The diffusion-prepared DTI sequence includes a diffusion-preparation module followed by 3D fast GRE. To minimize eddy current–related artifacts and to reduce T1 effects during readout, a stimulated-echo scheme (12,16) was adopted in diffusion-prepared DTI. Removable dental braces (Fig 2) with bonding trays were used so that MRI scans could be acquired with braces and without braces in the same participants. Five examinations were performed in each participant with an Ingenia 3.0-T MRI scanner (Philips Healthcare, Best, the Netherlands): MPRAGE, two-dimensional GRE EPI BOLD functional MRI, 3D T2-prepared BOLD functional MRI (repetition time, 2 sec; voxel size, $3.75 \times 3.75 \times 4$ mm^3), two-dimensional spin-echo (SE) EPI DTI, and 3D diffusion-prepared DTI (voxel size, $2.5 \times 2.5 \times 2.5$ mm^3). The examination order was chosen to be unique for each participant to avoid potential systematic biases. Optimized higher order shims using the toolbox described in Schär et al (17) and distortion correction (provided by the vendor) were applied in all EPI examinations. To assess BOLD functional MRI changes in the entire brain, a breath-hold task (4) was performed. A respiratory belt was placed around the participant's chest during the examinations. The point spread function was measured for each method (18).

Functional MRI data were analyzed by using statistical parametric mapping (SPM, version 12; Wellcome Trust Center for Neuroimaging, London, United Kingdom; *https://www.fil.ion.ucl.ac.uk/spm/*) and Matlab 2017a (MathWorks, Natick, Mass). Preprocessing steps include realignment, slice timing correction, coregistration, segmentation, and normalization. A general linear model was used to help detect functional

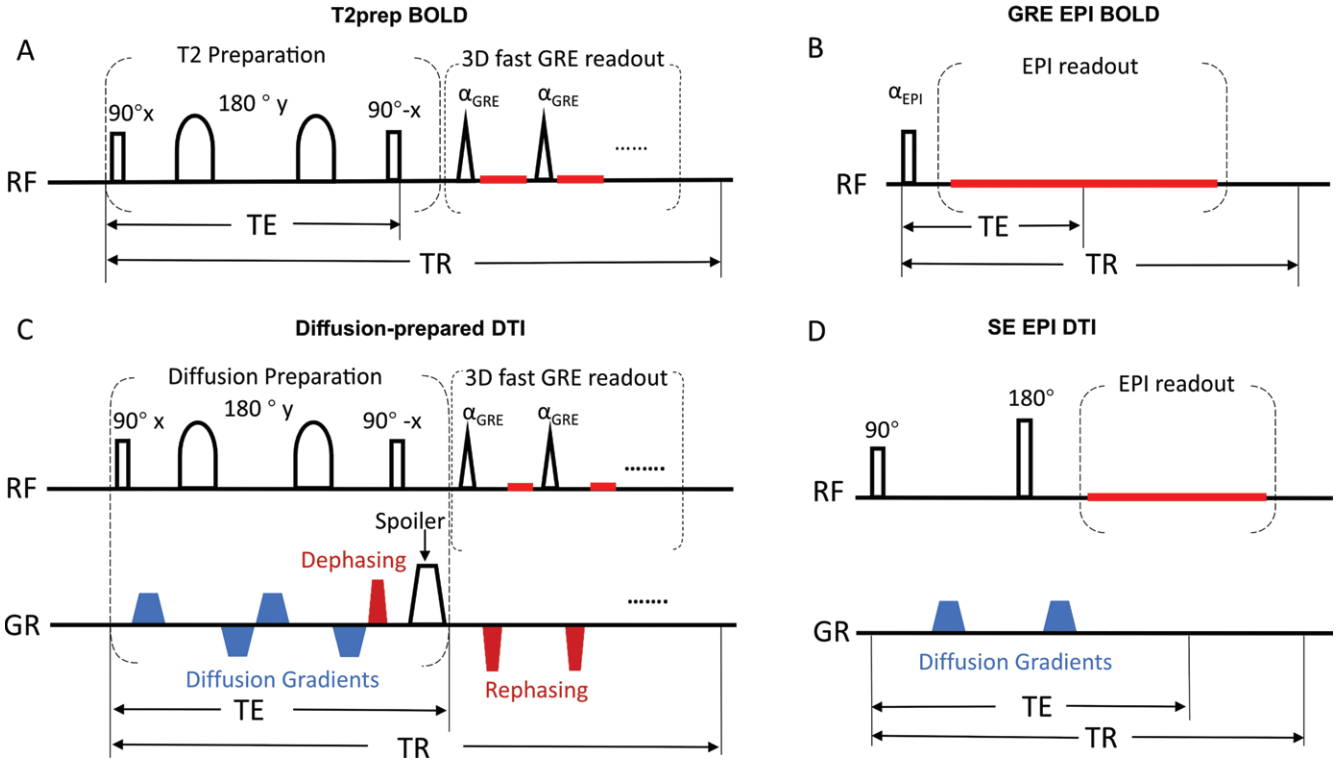

Figure 1: Image shows pulse sequence diagrams of, *A*, three-dimensional (3D) T2-prepared (T2prep) blood oxygenation level–dependent (BOLD) functional MRI, *B*, conventional two-dimensional multislice gradient-echo (GR) echo-planar imaging (EPI) BOLD functional MRI, *C*, 3D diffusion-prepared diffusion tensor imaging (DTI), and, *D*, conventional 2D multislice spin-echo (SE) EPI DTI. One entire image volume was acquired in a single repetition time (TR) period in all sequences to avoid well-known phase errors in multishot approaches. Details of these pulse sequences are described in Appendix E1 (online). RF = radiofrequency, TE = echo time.

Figure 2: Photograph shows custom-made dental braces that can be easily mounted on and removed from participants' teeth. Brackets made of stainless steel are bonded to a pair of indirect bonding trays made of hard plastic. Beta titanium archwire is seated and secured in bracket slots.

activation (adjusted $P < .05$, cluster size ≥3). Motion parameters recorded from the respiratory belt were regressed out. Functional MRI results were compared in two manually delineated regions of interest in each participant: one with strong susceptibility artifacts (dropout) and one covering bilateral motor cortex with minimal susceptibility artifacts at EPI.

DTI data were processed by using MRI Studio (*https://www.mristudio.org*). Signal-to-noise ratio (SNR), apparent diffusion coefficient, and fractional anisotropy were compared in two manually drawn regions of interest: bilateral inferior fronto-occipital fasciculus with strong susceptibility artifacts and bilateral posterior limb of internal capsule with minimal susceptibility artifacts at EPI. Geometric distortion on diffusion tensor images was visualized by using Slicer of FSL (version 6.0; *https://fsl.fmrib.ox.ac.uk/*) and quantified by using the Jaccard index that ranges from zero to one, indicating no overlap to complete agreement, respectively, between the geometric shapes of the diffusion tensor image and reference structural images.

Statistical Analysis

The sample size was determined from power analysis by using the approach described by Cohen et al (19) based on the average effect size (approximately 1.3) reported in previous studies (8) with power of 0.8 and significance set at $\alpha = .05$ (type I error, two tailed).

Paired *t* tests were performed to compare the results from respective functional MRI and DTI methods. More details on MRI pulse sequences, data analysis, and dental braces are provided in Appendix E1 (online).

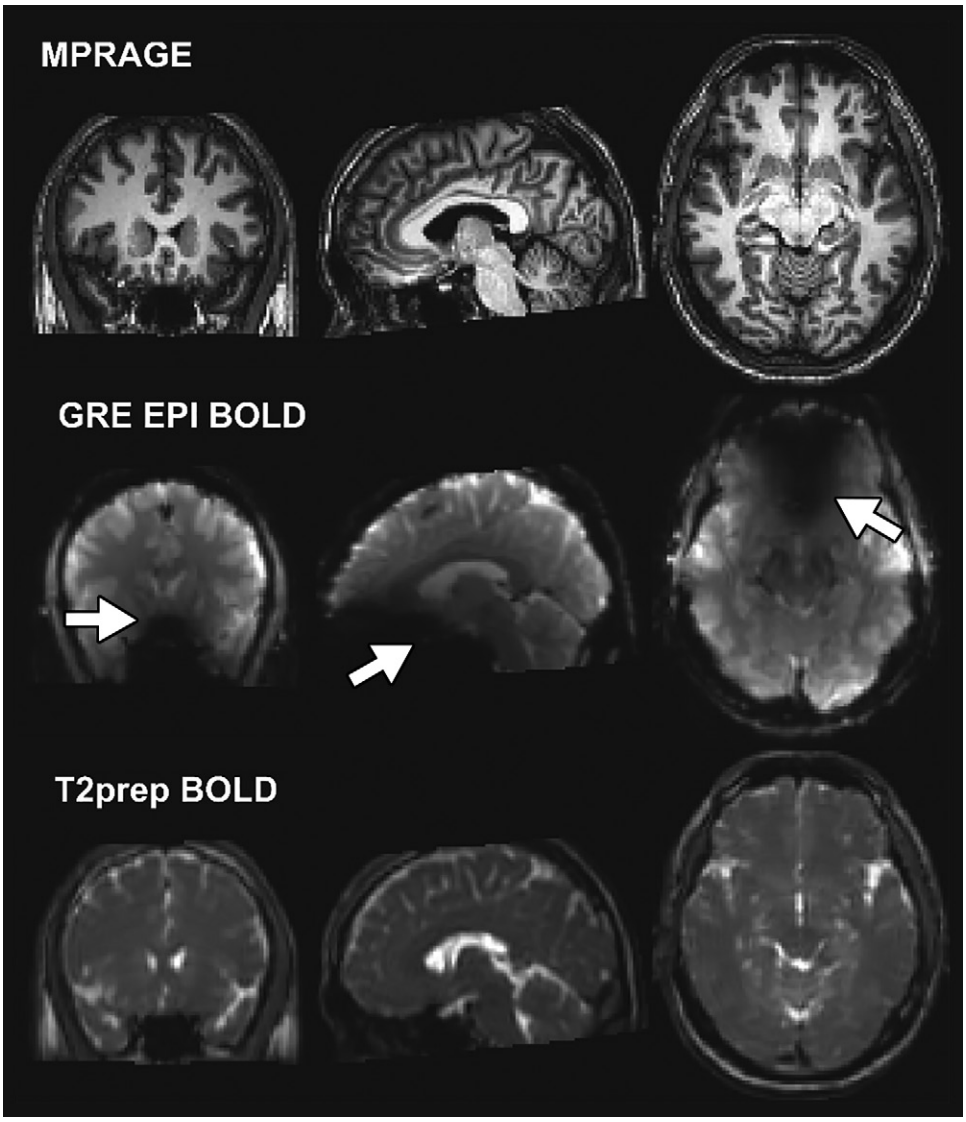

Figure 3: Representative anatomic (magnetization-prepared rapid acquisition gradient-echo [MPRAGE]), gradient-echo (GRE) echo-planar imaging (EPI) blood oxygenation level–dependent (BOLD), and T2-prepared (T2prep) BOLD images acquired in participant wearing titanium dental brace at 3.0 T. Image plane from left to right: coronal, sagittal, and axial. Signal dropouts can be seen on EPI-based images in regions close to brace (arrows). T2-prepared BOLD images were not affected by strong susceptibility effect.

Results

Study Participants

Six healthy participants (mean age ± standard deviation, 40 years ± 6; three women) were recruited for this study. Each participant underwent a 60-minute MRI session.

Functional MRI Results

Figure 3 demonstrates representative functional MRIs from one participant wearing braces. Large signal voids are seen on GRE EPI BOLD functional MRI scans, mainly in the orbitofrontal and ventromedial prefrontal cortex (subsequently defined as the dropout region). Little artifact was visible in the entire brain on MPRAGE and T2-prepared BOLD functional MRI scans. Typical activation maps during breath hold are shown in Figure 4. While activation was detected in most regions with minimal susceptibility artifacts using both methods, fewer activations were detected in the dropout region with GRE EPI BOLD than with T2-prepared BOLD functional MRI.

Quantitative Comparison: T2-prepared BOLD Functional MRI versus GRE EPI BOLD Functional MRI

The group-averaged quantitative results from all participants (n = 6) are summarized in Table 1. In the dropout region, temporal SNR, percentage signal change, and contrast-to-noise ratio were all significantly higher with T2-prepared BOLD functional MRI than with GRE EPI. In the motor cortex with minimal susceptibility artifacts, GRE EPI BOLD showed slightly higher (not significant) temporal SNR (P = .05), percentage signal change (P = .56), and contrast-to-noise ratio (P = .21) than did T2-prepared BOLD functional MRI. When the examinations were repeated without braces, temporal SNR, percentage signal change, and contrast-to-noise ratio in both the dropout and motor regions were slightly higher (not significant; dropout region: P = .06, P = .33, P = .06; motor region: P = .10, P = .91, P = .18) with GRE EPI BOLD functional MRI than with T2-prepared BOLD functional MRI.

Quantitative Comparison: Functional MRI with Braces versus without Braces

Temporal SNR, percentage signal change, and contrast-to-noise ratio in the dropout region were not significantly different with braces and without braces in T2-prepared BOLD

Figure 4: Activation maps overlaid on original functional MRI scans from, *A*, gradient-echo echo-planar imaging (EPI) and, *B*, T2-prepared (T2prep) blood oxygenation level–dependent functional MRI approaches, respectively, in axial imaging plane from healthy participant wearing titanium dental braces during breath-hold task. Activated voxels are highlighted with their corresponding *t* scores from general linear model analysis with identical statistical threshold. Range of *t* scores is indicated by scale bar.

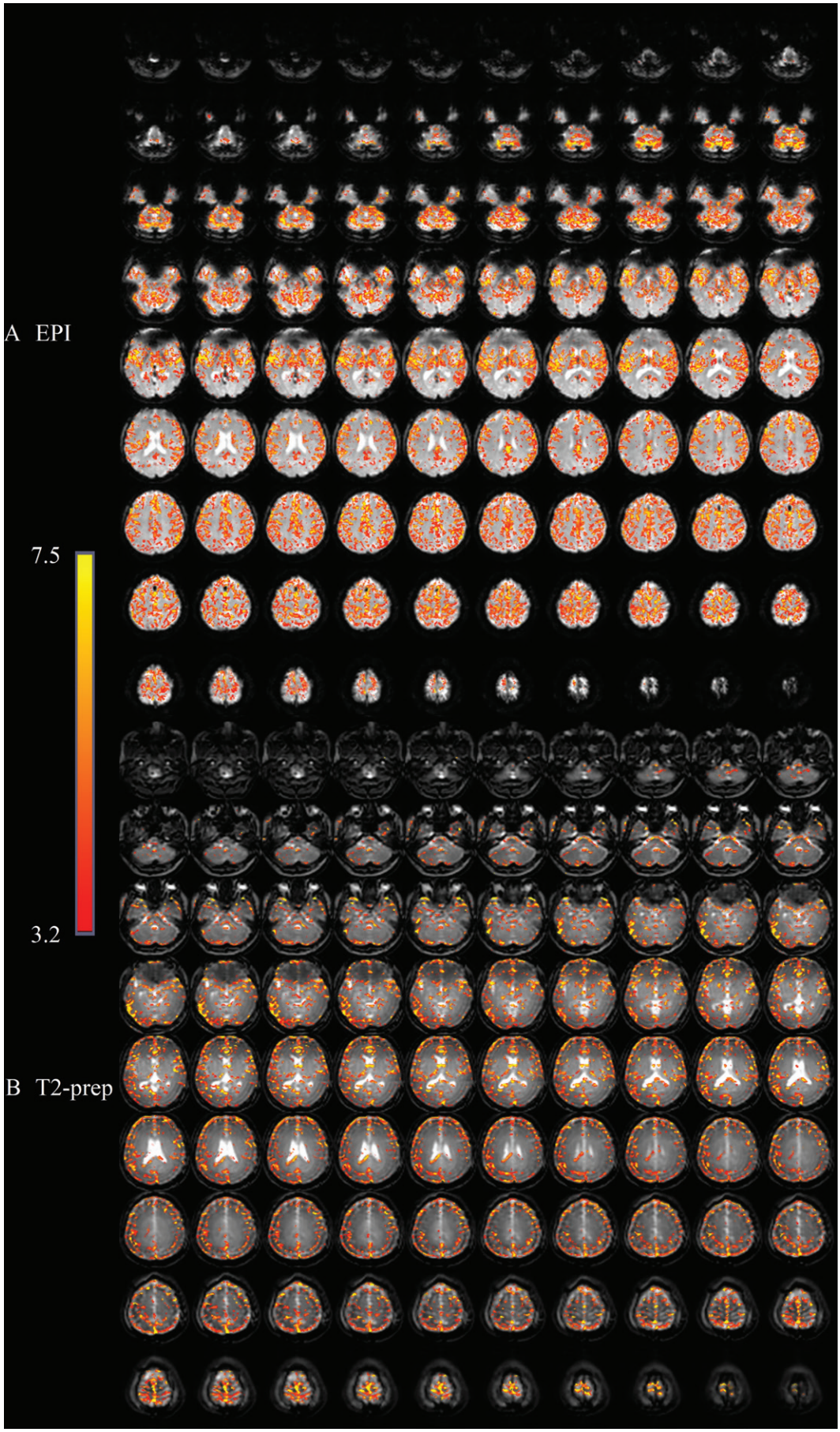
A EPI
7.5
3.2
B T2-prep

Table 1: Group-averaged Quantitative Results from All Participants (*n* = 6) for Comparison of the GRE EPI BOLD and T2-prepared BOLD Functional MRI Approaches

Parameter	Temporal Signal-to-Noise Ratio	Percentage Signal Change	Contrast-to-Noise Ratio
With braces			
Dropout region*			
T2-prepared	37.8 ± 2.4	2.3 ± 0.7	0.83 ± 0.16
EPI	15.5 ± 5.3	1.8 ± 0.23	0.29 ± 0.10
P value†	<.001	<.001	<.001
Motor cortex			
T2-prepared	41.6 ± 5.9	2.4 ± 0.7	1.1 ± 0.5
EPI	48.9 ± 7.6	2.6 ± 0.4	1.4 ± 0.4
P value	.05	.56	.21
Without braces			
Dropout region			
T2-prepared	37.0 ± 2.5	2.93 ± 0.54	1.1 ± 0.1
EPI	45.3 ± 6.3	2.83 ± 0.43	1.3 ± 0.2
P value	0.06	0.33	0.06
Motor cortex			
T2-prepared	44.4 ± 2.2	2.8 ± 0.6	1.3 ± 0.6
EPI	52.8 ± 5.8	2.8 ± 0.4	1.5 ± 0.1
P value	0.10	0.91	0.18

Note.—Unless otherwise specified, data are means ± standard deviation. Percentage signal change is relative signal change between breath hold and normal breathing. More details are described in Methods and Appendix E1 (online). BOLD = blood oxygenation level dependent, EPI = echo-planar imaging, GRE = gradient echo.

* Dropout region refers to the area showing large signal wipeout in echo-planar images in participants wearing metallic dental braces, which mainly includes the orbitofrontal and ventromedial prefrontal cortex.

† $P < .05$.

functional MRI ($P = .38$, $P = .18$, $P = .14$), but were significantly improved with GRE EPI BOLD without braces (Table E1 [online]). The results in the motor cortex in each method were not significantly different with braces and without braces (T2-prepared BOLD functional MRI: $P = .22$, $P = .47$, $P = .17$; GRE EPI BOLD: $P = .20$, $P = .27$, $P = .19$).

DTI Results

Figure 5 demonstrates typical raw diffusion-weighted images, apparent diffusion coefficient, and color-coded fractional anisotropy maps from one participant wearing braces. On diffusion-weighted images and apparent diffusion coefficient maps, no obvious artifact was visible in diffusion-prepared DTI in the entire brain, whereas susceptibility artifacts were substantial in SE EPI DTI. Fractional anisotropy maps color-coded by V1 orientation from SE EPI DTI showed spurious results in the inferior frontal lobe near the braces, affecting visualization of the inferior fronto-occipital fasciculus. Compared with MPRAGE, geometric distortion (Fig 6) was minimal in diffusion-prepared DTI, but was substantial in SE EPI DTI (significantly lower Jaccard index in each slice; $P < .001$). The degree of distortion (Jaccard index) in SE EPI DTI varied with the location of slice. However, diffusion-prepared diffusion tensor images appeared smoother than did SE EPI diffusion tensor images.

Quantitative Comparison: Diffusion-prepared DTI versus SE EPI DTI

Table 2 summarizes the group-averaged quantitative DTI results from all participants ($n = 6$). Apparent diffusion coefficient ($P = .88$) and fractional anisotropy ($P = .33$) were not significantly different between diffusion-prepared DTI and SE EPI DTI, and SNR was slightly higher in SE EPI DTI (not significant; $P = .05$) in the posterior limb of internal capsule with minimal susceptibility artifacts. In the inferior fronto-occipital fasciculus close to the braces, SNR was significantly diminished in SE EPI DTI, leading to suspicious apparent diffusion coefficient and fractional anisotropy, whereas diffusion-prepared DTI showed greater SNR and reasonable apparent diffusion coefficient and fractional anisotropy consistent with the literature (20). When the examinations were repeated without braces, apparent diffusion coefficient, fractional anisotropy, and SNR in both posterior limb of internal capsule ($P = .52$, $P = .11$, $P = .45$) and inferior fronto-occipital fasciculus ($P = .77$, $P = .19$, $P = .27$) became not significantly different between SE EPI DTI and diffusion-prepared DTI.

Quantitative Comparison: DTI with Braces versus DTI without Braces

Apparent diffusion coefficient, fractional anisotropy, and SNR in inferior fronto-occipital fasciculus were not significantly different with braces and without braces in diffusion-prepared DTI ($P = .37$, $P = .35$, $P = .43$), but were significantly improved in SE EPI DTI without braces (Table E2 [online]). The results in posterior limb of internal capsule in each method were not significantly different with braces and without braces (diffusion prepared DTI: $P = .17$, $P = .33$, $P = .28$; SE EPI DTI: $P = .21$, $P = .23$, $P = .31$).

Point Spread Function

The full width at half maximum, or FWHM, of point spread function was not significantly different between 3D T2-prepared BOLD functional MRI (readout × phase-encoding – y × phase-encoding – z = 7.3 mm × 7.4 mm × 7.7 mm) and two-dimensional GRE EPI BOLD functional MRI (readout × phase-encoding – y = 7.3 mm × 7.6 mm). The FWHM for 3D diffusion-prepared DTI with stimulated echo (5.7 mm × 6.5 mm × 6.7 mm) and two-dimensional SE EPI DTI (5.5 mm ×

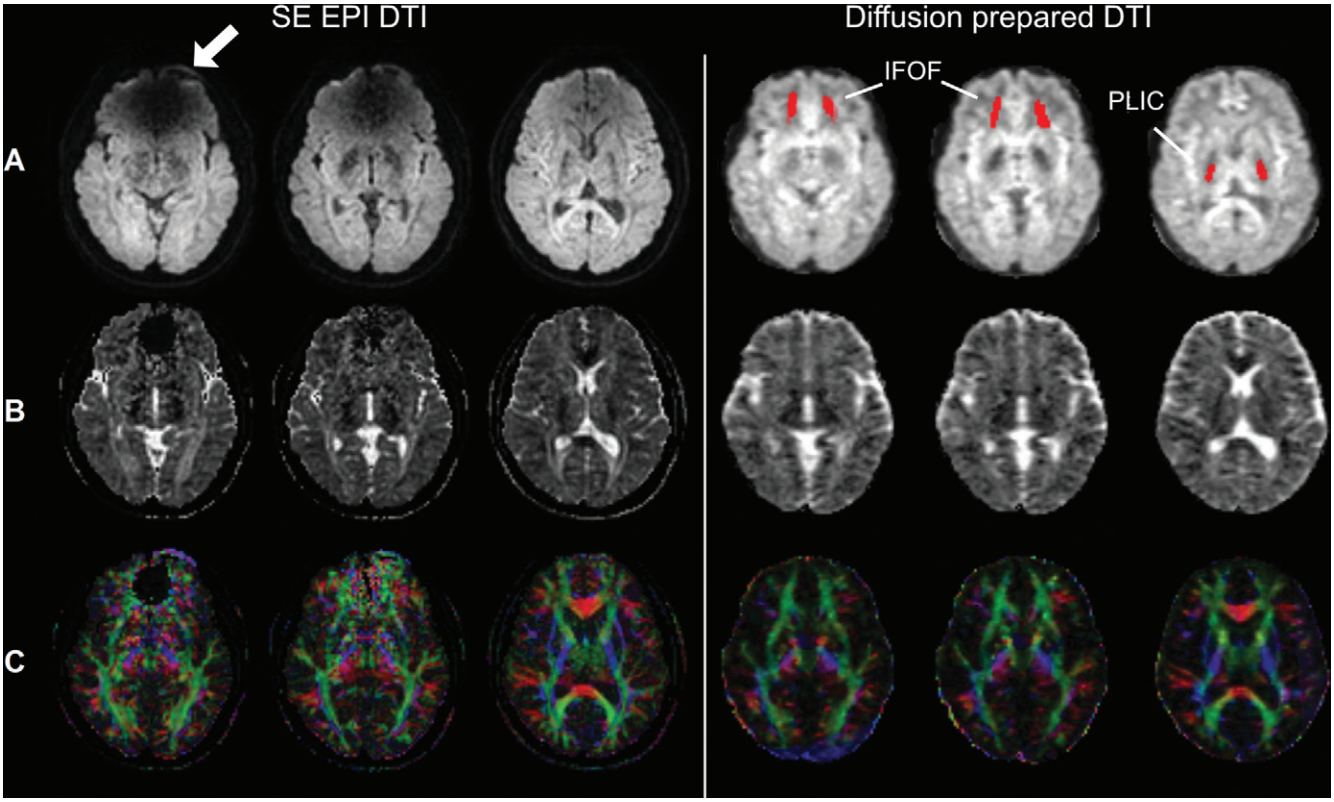

Figure 5: Spin-echo (SE) echo-planar imaging (EPI) and diffusion-prepared diffusion tensor imaging (DTI) axial images acquired at 3.0 T in participant wearing metallic dental braces. *A*, Raw diffusion-weighted images, *B*, calculated apparent diffusion coefficient maps, and, *C*, fractional anisotropy map color coded by V1 (principal eigenvector) orientation (standard red, green, and blue convention). Susceptibility artifacts were observed on SE echo-planar image in regions close to braces (arrow). No obvious artifacts were seen on diffusion-prepared diffusion tensor image. Regions of interest of inferior fronto-occipital fasciculus (IFOF) and posterior limb of internal capsule (PLIC) used in subsequent quantitative analysis are highlighted on diffusion-prepared diffusion tensor images with red.

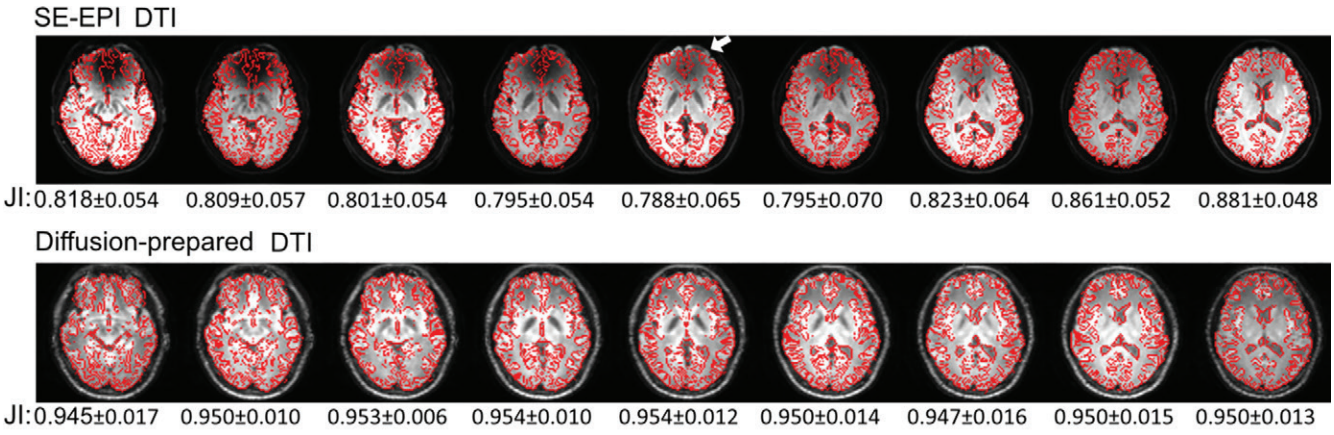

Figure 6: Geometric distortion in axial spin-echo (SE) echo-planar imaging (EPI) (top row) and diffusion-prepared (bottom row) diffusion tensor images when compared with anatomic magnetization-prepared rapid acquisition gradient-echo (MPRAGE) images in same participant wearing metallic dental braces. Edges of brain structures obtained from coregistered MPRAGE images are shown in red contour lines on mean diffusion-weighted images from corresponding diffusion tensor imaging (DTI) approaches. Mismatch between red contour lines and edge of structures shown in diffusion tensor images illustrates geometric distortion artifacts (eg, in frontal area indicated by arrow). Mean Jaccard index (JI) is calculated for each slice and is listed under each image. SE EPI DTI showed significantly lower JI in each corresponding slice ($P < .01$).

5.2 mm) was not significantly different on the readout direction, but it was approximately 25% wider on the first phase-encoding direction in diffusion-prepared DTI. The FWHM for diffusion-prepared DTI without stimulated echo was 5.7 mm × 5.3 mm × 5.5 mm, which was narrower on the phase-encoding directions than was diffusion-prepared DTI with stimulated echo.

Higher Spatial Resolution

We used relatively low spatial resolution here to match routine clinical examinations at 3.0 T and to compare the methods. Figure E1 (online) shows the feasibility for the proposed methods to acquire whole-brain images with a voxel size of 1.5 × 1.5 × 1.5 mm^3 at a field strength of 3.0 T.

Table 2: Group-averaged Quantitative Results from All Participants (*n* = 6) for Comparison of the Spin-Echo EPI and Diffusion-prepared DTI Approaches

Parameter	Signal-to-Noise Ratio	ADC (10^{-3}mm^2/sec)	Fractional Anisotropy
With braces			
Inferior fronto-occipital fasciculus			
Diffusion-prepared	5.8 ± 1.5	0.75 ± 0.08	0.45 ± 0.07
Spin-echo EPI	3.8 ± 0.7	0.16 ± 0.16	0.10 ± 0.12
P value*	.03	<.001	<.001
Posterior limb of the internal capsule			
Diffusion-prepared	5.7 ± 1.1	0.73 ± 0.04	0.61 ± 0.03
Spin-echo EPI	7.0 ± 1.3	0.72 ± 0.03	0.59 ± 0.05
P value	.05	.88	.33
Without braces			
Inferior fronto-occipital fasciculus			
Diffusion-prepared	5.8 ± 1.1	0.79 ± 0.23	0.49 ± 0.02
Spin-echo EPI	6.2 ± 0.5	0.80 ± 0.18	0.45 ± 0.01
P value	.27	.77	.19
Posterior limb of the internal capsule			
Diffusion-prepared	6.2 ± 1.6	0.68 ± 0.27	0.60 ± 0.01
Spin-echo EPI	7.0 ± 1.5	0.69 ± 0.20	0.58 ± 0.01
P value	.45	.52	.11

Note.— Unless otherwise specified, data are means ± standard deviation. More details are described in Methods and Appendix E1 (online). ADC = apparent diffusion coefficient, EPI = echo-planar imaging, DTI = diffusion tensor imaging.
* $P < .05$.

Discussion

Susceptibility artifacts caused by metallic objects at echo-planar imaging (EPI) have been a major limitation for functional MRI and diffusion tensor imaging (DTI) in participants wearing metallic orthodontic material and other head implants. This study was designed to evaluate the ability of two alternative approaches: T2-prepared blood oxygenation level–dependent (BOLD) functional MRI and diffusion-prepared DTI to reduce such susceptibility artifacts in healthy human participants wearing metallic orthodontic braces. T2-prepared BOLD functional MRI and diffusion-prepared DTI showed preserved signal-to-noise ratio (SNR) in the entire brain, whereas conventional EPI approaches showed significantly reduced SNR in regions with strong susceptibility effects (functional MRI: 37.8 ± 2.4 vs 15.5 ± 5.3, $P < .001$; DTI: 5.8 ± 1.5 vs 3.8 ± 0.7, $P = .03$). Because our main goal was to compare the two types of methods in the presence of metallic dental braces, a breath-hold task was chosen as a simple and robust whole-brain functional MRI stimulation. The functional MRI approaches have also been evaluated in other tasks, including language mapping in presurgical patients (6,8).

SE echo-planar images have less signal dropout than do GRE echo-planar images as signal dropouts caused by through-plane susceptibility gradients are refocused. However, dropouts can still occur at SE EPI due to in-plane susceptibility gradients (21) and B1 inhomogeneity, as shown in our SE EPI DTI data with orthodontic braces. Even when complete dropout is avoided, in-plane susceptibility gradients can cause nonlinear distortion that is difficult to correct for (often needing additional DTI examinations with opposite phase-encoding direction [22]), signal reduction (thus compromising SNR), and erroneous diffusion measures (23). We showed substantially reduced distortion throughout the brain in T2-prepared BOLD functional MRI and diffusion-prepared DTI compared with EPI.

For functional MRI, the T2*-weighted GRE BOLD contrast detected with GRE EPI is more sensitive to the BOLD effect than the T2-weighted SE BOLD contrast measured in T2-prepared BOLD when susceptibility artifacts are minimal. However, when susceptibility artifacts became prominent, the BOLD sensitivity dropped substantially with GRE EPI, but was largely preserved in the entire brain in T2-prepared BOLD functional MRI. Our data showed that compared with GRE EPI, contrast-to-noise ratio in T2-prepared BOLD functional MRI was 15%–25% lower in the motor cortex (minimal susceptibility artifacts) but was greater than 150% higher in regions affected by the braces. SE EPI BOLD is another commonly used T2-weighted SE BOLD approach. A quantitative comparison between SE EPI BOLD and T2-prepared BOLD functional MRI was performed previously (6). However, unlike GRE EPI BOLD, SE EPI BOLD is rarely used clinically due to its high-power deposition and other limitations (6). We are currently developing a T2*-prepared BOLD functional MRI method.

The stimulated-echo scheme (12,16) used in diffusion-prepared DTI halves signal intensity compared with the same sequence without stimulated echo. Therefore, compared with SE EPI DTI, SNR in diffusion-prepared DTI was 10%–20% lower in regions with minimal susceptibility artifacts, but was 40%–50% higher in regions affected by the braces. Another drawback is that diffusion-prepared diffusion tensor images appear smoother than do SE EPI diffusion tensor images; this is a result of the widened point spread function on phase-encoding direction mainly caused by a longer echo train due to the dephasing and rephrasing gradients needed to generate the stimulated echo. This is supported by our point spread function measurement with and without the stimulated-echo scheme. However, the stimulated-echo scheme is important to suppress eddy-current artifacts and T1-relaxation effects that can cause erroneous diffusion measures (12,16), which we think outweigh the relatively minor loss in SNR and spatial resolution.

There are a wide variety of materials that constitute orthodontic braces (24,25) and other head implants. Therefore, our results

should be extrapolated with caution to implants made with different materials. When the susceptibility gradients exceed the readout bandwidth of 3D fast GRE, significant dropouts will still be present. The readout bandwidth with 3D fast GRE is typically much higher (>500 Hz/pixel) than with EPI (<100 Hz/pixel, phase-encoding direction). For materials with difference in susceptibility (with respect to water) less than 30 ppm (1) (eg, most alloys of precious metals in electrodes for deep brain stimulation or electroencephalography), 3D fast GRE can provide whole-brain largely artifact-free images (1). For materials with difference in susceptibility (with respect to water) less than 1500 ppm (1) (eg, titanium [about 200 ppm], gold [about −25 ppm], nickel [about 125 ppm]), 3D fast GRE typically shows no susceptibility artifact in regions greater than 20 mm from the implants (1–3). The distance between teeth and brain is usually greater than 50 mm in adults. In children or adolescents with orthodontic material, the distance is shorter, but should still be well above 20 mm. However, in regions immediately surrounding such materials, multispectral imaging (26) may be the only existing MRI technique to reduce such near-metal artifacts.

There were limitations to our study. The contrasts induced in the preparation modules decrease during the 3D fast GRE echo train. To minimize this effect, a centric phase-encoding profile was used in 3D fast GRE, in which the center of k-space, which determines the gross signal intensity in MRI scans, is acquired immediately after the preparation modules when the target contrast is strongest. The contrasts for higher spatial frequencies, such as the boundaries between cerebrospinal fluid and tissue, are smaller. Parallel imaging techniques can substantially shorten the 3D fast GRE echo train and thus reduce this effect. We showed that high-spatial-resolution whole-brain images can be acquired with the proposed methods by using advanced parallel imaging techniques. Finally, the results were evaluated in a small number of healthy participants without pathologic findings, which posed another limitation and warrants further investigation.

In summary, our results showed that T2-prepared blood oxygenation level–dependent functional MRI and diffusion-prepared diffusion tensor imaging can be useful alternatives for human brain mapping when echo-planar imaging fails to provide robust signals in the presence of metallic implants such as dental braces.

Acknowledgments: The authors thank the staff in the F.M. Kirby Research Center for Functional Brain Imaging at the Kennedy Krieger Institute for experimental assistance. Equipment used in the study was manufactured by Philips Healthcare.

Author contributions: Guarantors of integrity of entire study, Y.W., J.H.; study concepts/study design or data acquisition or data analysis/interpretation, all authors; manuscript drafting or manuscript revision for important intellectual content, all authors; approval of final version of submitted manuscript, all authors; agrees to ensure any questions related to the work are appropriately resolved, all authors; literature research, X.M., Y.W., D.L., D.W., R.D.A., Q.Q., J.J.P., J.H.; clinical studies, X.M., Y.W., D.L., H.J., J.H.; statistical analysis, X.M., H.J., N.I.S.B., J.H.; and manuscript editing, X.M., R.D.A., C.B., K.S.R., Q.Q., P.C.M.v.Z., J.J.P., J.H.

Disclosures of Conflicts of Interest: **X.M.** disclosed no relevant relationships. **Y.W.** disclosed no relevant relationships. **D.L.** disclosed no relevant relationships. **H.J.** Activities related to the present article: disclosed no relevant relationships. Activities not related to the present article: is employed by Johns Hopkins University; has grants/grants pending with National Institutes of Health (NIH). Other relationships: disclosed no relevant relationships. **D.W.** disclosed no relevant relationships. **M.T.S.** disclosed no relevant relationships. **N.I.S.B.** disclosed no relevant relationships. **R.D.A.** disclosed no relevant relationships. **C.B.** Activities related to the present article: disclosed no relevant relationships. Activities not related to the present article: is a consultant for Depuy-Synthes. Other relationships: disclosed no relevant relationships. **K.S.R.** disclosed no relevant relationships. **Q.Q.** disclosed no relevant relationships. **P.C.M.v.Z.** Activities related to the present article: disclosed no relevant relationships. Activities not related to the present article: is member of editorial board for Elsevier; has grants/grants pending with NIH and Philips Healthcare; received payment for lectures including service on speakers bureaus from Philips Healthcare and has technology licensed to them (this arrangement has been approved by Johns Hopkins University in accordance with its conflict of interest policies); has patents (planned, pending, or issued) with and receives royalties from Philips Healthcare and Siemens; received payment for travel/accommodations/meeting expenses unrelated to activities listed. Other relationships: disclosed no relevant relationships. **J.J.P.** Activities related to the present article: disclosed no relevant relationships. Activities not related to the present article: receives royalties from Elsevier and Springer Science & Business Media. Other relationships: disclosed no relevant relationships. **J.H.** disclosed no relevant relationships.

References

1. Starcuková J, Starčuk Z Jr, Hubálková H, Linetskiy I. Magnetic susceptibility and electrical conductivity of metallic dental materials and their impact on MR imaging artifacts. Dent Mater 2008;24(6):715–723.
2. New PF, Rosen BR, Brady TJ, et al. Potential hazards and artifacts of ferromagnetic and nonferromagnetic surgical and dental materials and devices in nuclear magnetic resonance imaging. Radiology 1983;147(1):139–148.
3. Hinshaw DB Jr, Holshouser BA, Engstrom HI, Tjan AH, Christiansen EL, Catelli WF. Dental material artifacts on MR images. Radiology 1988;166(3):777–779.
4. Zaca D, Hua J, Pillai JJ. Cerebrovascular reactivity mapping for brain tumor presurgical planning. World J Clin Oncol 2011;2(7):289–298.
5. Stippich C, ed. Clinical Functional MRI: Presurgical Functional Neuroimaging. 2nd ed. Berlin, Germany: Springer, 2015.
6. Hua J, Qin Q, van Zijl PCM, Pekar JJ, Jones CK. Whole-brain three-dimensional T2-weighted BOLD functional magnetic resonance imaging at 7 Tesla. Magn Reson Med 2014;72(6):1530–1540.
7. Parrish T, Hu X. A new T2 preparation technique for ultrafast gradient-echo sequence. Magn Reson Med 1994;32(5):652–657.
8. Hua J, Miao X, Agarwal S, et al. Language Mapping Using T2-Prepared BOLD Functional MRI in the Presence of Large Susceptibility Artifacts-Initial Results in Patients With Brain Tumor and Epilepsy. Tomography 2017;3(2):105–113.
9. Agarwal S, Hua J, Sair HI, et al. Repeatability of language fMRI lateralization and localization metrics in brain tumor patients. Hum Brain Mapp 2018;39(12):4733–4742.
10. Lee H, Price RR. Diffusion imaging with the MP-RAGE sequence. J Magn Reson Imaging 1994;4(6):837–842.
11. Sinha U, Sinha S. High speed diffusion imaging in the presence of eddy currents. J Magn Reson Imaging 1996;6(4):657–666.
12. Zhang Q, Coolen BF, Versluis MJ, Strijkers GJ, Nederveen AJ. Diffusion-prepared stimulated-echo turbo spin echo (DPsti-TSE): An eddy current-insensitive sequence for three-dimensional high-resolution and undistorted diffusion-weighted imaging. NMR Biomed 2017;30(7):e3719.
13. Jeong EK, Kim SE, Parker DL. High-resolution diffusion-weighted 3D MRI, using diffusion-weighted driven-equilibrium (DW-DE) and multishot segmented 3D-SSFP without navigator echoes. Magn Reson Med 2003;50(4):821–829.
14. Hiwatashi A, Togao O, Yamashita K, et al. Evaluation of diffusivity in pituitary adenoma: 3D turbo field echo with diffusion-sensitized driven-equilibrium preparation. Br J Radiol 2016;89(1063):20150755.
15. Shellock FG. Reference Manual for Magnetic Resonance Safety, Implants, and Devices. Playa del Rey, Calif: Biomedical Research Publishing Group, 2014.
16. Gibbs SJ, Carpenter TA, Hall LD. Diffusion imaging with unshielded gradients. J Magn Reson 1992;98(1):183–191.
17. Schär M, Kozerke S, Fischer SE, Boesiger P. Cardiac SSFP imaging at 3 Tesla. Magn Reson Med 2004;51(4):799–806.
18. Robson MD, Gore JC, Constable RT. Measurement of the point spread function in MRI using constant time imaging. Magn Reson Med 1997;38(5):733–740.
19. Cohen J. Statistical Power Analysis for the Behavioral Sciences. Hillsdale, NJ: L. Erlbaum Associates, 1988.
20. Mori S. Introduction to diffusion tensor imaging. Amsterdam, the Netherlands: Elsevier, 2007.
21. Turner R, Ordidge RJ. Technical challenges of functional magnetic resonance imaging. IEEE Eng Med Biol Mag 2000;19(5):42–54.
22. Sotiropoulos SN, Jbabdi S, Xu J, et al. Advances in diffusion MRI acquisition and processing in the Human Connectome Project. Neuroimage 2013;80:125–143.
23. Goto M, Abe O, Hata J, et al. Adverse effects of metallic artifacts on voxel-wise analysis and tract-based spatial statistics in diffusion tensor imaging. Acta Radiol 2017;58(2):211–217.
24. Costa ALF, Appenzeller S, Yasuda CL, Pereira FR, Zanardi VA, Cendes F. Artifacts in brain magnetic resonance imaging due to metallic dental objects. Med Oral Patol Oral Cir Bucal 2009;14(6):E278–E282.
25. Wylezinska M, Pinkstone M, Hay N, Scott AD, Birch MJ, Miquel ME. Impact of orthodontic appliances on the quality of craniofacial anatomical magnetic resonance imaging and real-time speech imaging. Eur J Orthod 2015;37(6):610–617.
26. Lu W, Pauly KB, Gold GE, Pauly JM, Hargreaves BA. SEMAC: Slice encoding for metal artifact correction in MRI. Magn Reson Med 2009;62(1):66–76.